Cross sections and other parameters of $e^- - H_2O$ scattering $(E_i \geqslant 50\,\text{eV})$

K N JOSHIPURA and MINAXI VINODKUMAR*

Department of Physics, Sardar Patel University, Vallabh Vidyanagar, Gujarat 388 120, India
*V. P. & R. P. T. P. Science College, Vallabh Vidyanagar, Gujarat 388 120, India

Abstract. Our previous theoretical work on $e^- - H_2O$ scattering has been modified and extended to intermediate and high energies E_i. Using the Bethe plot, we compare the present inelastic cross-sections with the experimental ionization cross sections. Total cross-sections are analytically represented as $Q_{\text{TOT}}(\text{cm}^2) = a.(E_i\,\text{eV})^{-b}$ and the parameters 'a' and 'b' are discussed for molecules H_2O, NH_3 and CH_4 in the range $E_i = 100$–$1000\,\text{eV}$.

Keywords. Electron-molecule scattering; total cross-sections; Bethe plot.

PACS No. 34·80

1. Introduction

Collisions of electrons with water molecules have been the target of theoretical and experimental investigation since long. Our recent paper [1], hereafter referred to as paper I, dealt with calculations on vibrationally elastic $e^- - H_2O$ scattering at intermediate energies $E_i = 10$–$300\,\text{eV}$. We treated the $e^- - H_2O$ interaction potentials in spherical models and the nonspherical interaction, mainly the molecular dipole potential was treated separately. The overall effect of electronic excitation and ionization was included through the imaginary part [2] of the complex spherical optical potential. All the terms of this complex potential were constructed by starting with an accurate spherically averaged charge density of the target molecule. A number of experimental results are also available for various cross-sections of the $e^- - H_2O$ system [3, 4]. Our total cross-sections given in paper I are in agreement with the experimental results of Sueoka et al [3] which in turn, are on the lower side of a number of other measurements e.g., those of Zecca et al [4]. Further, paper I demonstrated that it is more appropriate to consider the target charge density to be distorted dynamically by the polarization effect of the projectile.

In the present paper, two corrections have been introduced over the previous work. The absorption potential of Staszewska et al [2] V_{abs} vanishes at or below the threshold of electronic excitation Δ_{gap}. Paper I employed $\Delta_{\text{gap}} = I$, the ionization energy of H_2O which is $12\cdot6\,\text{eV}$. More appropriately Δ_{gap} should correspond to the actual energy of excitation to the (first or low-lying) electronic energy level of the target. Presently, we have considered $\Delta_{\text{gap}} = 10\cdot2\,\text{eV}$ which is the excitation energy for the important transition $X^1A_1 \to {}^3A_1$ in H_2O (see ref. [5]). Further the Bethe plot of our total

inelastic cross-sections Q_{inel} is also given here. This now compares meaningfully well with the experimental ionization cross-sections $Q(H_2O^+)$.

Secondly the vibrational excitation cross-sections calculated recently by Nishimura and Itikawa [6] though important at low and intermediate energies only, may be added incoherently to define the grand total cross-sections. Thus the present work incorporates these two changes and reports grand total cross-sections Q_{TOT} at intermediate and high energies $E_i = 50\text{--}2000\,\text{eV}$. We have also discussed here the scaling laws, or the fitting formulas to investigate the functional dependence of cross-sections on incident energy, especially, above $100\,\text{eV}$. A comparison in this regard has also been made with other 10-electron systems viz., CH_4 and NH_3. A consistent picture of E_i-dependence of Q_{TOT} emerges for all the three 10-electron systems. Theoretical expressions in this paper are given in a.u., unless specified otherwise.

2. Theoretical aspects

Potentials and scattering calculations

Katase *et al* [7] have given a simple but accurate spherical single-centre charge-density of H_2O in the form

$$\rho_0(r) = \frac{1}{4\pi}\left[a_1 \exp\left(\frac{-r}{b_1}\right) + a_2 r \exp\left(\frac{-r}{b_2}\right) \right], \tag{1}$$

where $a_1 = 4478$, $a_2 = 125$, $b_1 = 0.0602$ and $b_2 = 0.322$.

Ab initio accurate charge-density of molecules can be calculated using quantum chemistry techniques. This allows for a proper treatment of correlation and exchange potentials of the electron-molecule system [8,9]. However, in the present case the model charge-density of (1) accurately reproduces the charge distribution in H_2O, given in refs [10–12]. It has a convenient form for carrying out the electron scattering calculations [1].

Considering $\rho_0(r)$ as the static or unperturbed charge-density of the target, we construct the dynamically distorted charge-density, as in [1]

$$\rho'(r, E_i) = \rho_0(r) + \rho_{\text{pol}}(r, E_i), \tag{2}$$

where ρ_{pol}, the polarized part of the charge-density based on the dynamic polarization potential is given by (5) and (7) of paper I. At high enough electron-energies ($\geqslant 500\,\text{eV}$), as the polarization effect dwindles, $\rho'(r, E_i)$ merges with $\rho_0(r)$, as expected. Now, the complex spherical optical potential of $e^- - H_2O$ system consists of static, exchange, polarization and absorption terms. Starting with (1) and (2) given here, we construct all the terms of the optical potential as in [1]. In particular the parameter Δ_{gap} in the V_{abs} of ref. [2] is now chosen to have a more realistic value $10.2\,\text{eV}$, as explained in § 1. This improvement is significant at intermediate energies (say $\leqslant 300\,\text{eV}$) only. Details of the scattering calculations are given in paper I and are not repeated here. We have calculated the total cross-sections for (elastic + inelastic) scattering viz.,

$$Q_T^S(E_i) = Q_{\text{el}}(E_i) + Q_{\text{inel}}(E_i), \tag{3}$$

where Q_{el} is the total elastic cross section within the complex potential. The superscript S in Q_T^S refers to the spherical interactions. The total inelastic cross section Q_{inel} shows the cumulative effect of all electronic excitations and the direct ionization, so that $Q_{inel} > Q(H_2O^+)$ at a particular E_i. Our model does not include dissociative ionization processes and vibrational and rotational excitations. The non-spherical dipole potential dominant at low to intermediate energies, was considered incoherently in [1]. Following this approach for the present energy range, we define the grand total cross-sections of $e^- - H_2O$ scattering, i.e.,

$$Q_{TOT}(E_i) = Q_T^S(E_i) + Q_{01}(D, E_i) + Q_{vib}(E_i). \tag{4}$$

We have followed paper I to obtain the dipole rotational excitation cross section $Q_{01}(D, E_i)$. These are the total cross-sections for the electron impact $0 \rightarrow 1$ rotational excitation, calculated in the Born approximation for the molecular dipole of strength D. The vibrationally inelastic integral cross-sections $Q_{vib}(E_i)$ determined by Nishimura and Itikawa [6] and included here are quite small for $E_i \geqslant 30$ eV.

The Bethe plot and the fitting formulas

It is well-known that at high energies the total inelastic cross-sections obey the Bethe asymptotic formula, as given by Inokuti [13]. This is

$$\frac{Q_{inel}}{4\pi a_0^2} \frac{E_i}{R} = (-M_{tot}^2) \ln\left(\frac{E_i}{R}\right) + M_{tot}^2 \ln[4C_{tot}] + O\left(\frac{R}{E_i}\right), \tag{5}$$

where a_0 is the Bohr-radius and R is the Rydberg unit of energy. The parameter M_{tot}^2 measuring the slope of the Bethe plot, is the square of the total dipole-matrix element. This formula is presently applied to our Q_{inel} results as well as to the total (direct) ionization cross-sections $Q(H_2O^+)$ recently measured by Srivastava [14].

We next consider the E_i-dependence of the total electron scattering cross-sections Q_{TOT} of H_2O vis-a-vis the other two well-known 10-electron molecules CH_4 and NH_3. Nishimura and Tawara [15] have given the following fitting formulas for CH_4 and other hydrocarbons, applicable to intermediate energies.

$$Q_{TOT} = \frac{a}{\sqrt{E_i}}. \tag{6a}$$

$$= b\sqrt{\frac{\alpha_0}{E_i}}. \tag{6b}$$

These two expressions, with 'a' and 'b' as typical molecular parameters and α_0 as the target polarizability, emphasize $E_i^{-1/2}$ dependence of the cross-sections in the range 50–500 eV.

Zecca *et al* [16] found that their measured values for NH_3, SiH_4 and H_2S targets are in accordance with the following formula, based on the Yukawa potential with the Born approximation, at $E_i > 200$ eV.

$$Q_{TOT}(E_i) = \frac{\sigma_0 B}{B + \sigma_0 E_i}. \tag{7}$$

The present theoretical results on H_2O are based on the partial wave analysis of the complex optical potential. This consists of short-range (static + exchange) potentials, intermediate range absorption potential and the long range polarization potential. Hence we have represented the grand-total cross-sections Q_{TOT}(in cm^2) in a general form, as a function of energy (eV), viz.,

$$Q_{TOT}(E_i) = a(E_i)^{-b},\qquad (8)$$

where '*a*' and '*b*' are our target-dependent parameters. This formula is found to be suitable for the present results in the range 100–1000 eV. Now, in order to apply (8) to the other 10-electron systems CH_4 and NH_3, we calculated their cross-sections through our modified additivity rule for e^--molecule scattering at high energies as given in [17]. Here the cross-sections of short-range atomic potentials in the molecule, i.e. $Q_{SR}(i)$ are added together and the long range (polarization) contribution $Q_{pol}(M)$ is considered at the direct molecular level. Thus, with '*n*' atoms in a molecule

$$Q_{TOT}(E_i) = \sum_{i=1}^{n} Q_{SR}(i) + Q_{pol}(M).\qquad (9)$$

This formulation goes over to the simple 'additivity rule' [18, 19] at high energies. The cross-sections of H_2O, CH_4 and NH_3 are found to have an identical E_i dependence, as discussed in the next section.

3. Results, discussion and conclusion

In a spherical model for H_2O, the total elastic cross-sections Q_{el} and the total inelastic cross-sections Q_{inel} are calculated to obtain $Q_T^S(E_i)$, vide eq. (3). The present values of Q_{inel} are somewhat higher (up to about 300 eV) than the previous values [1], in view of our choice of Δ_{gap}. The present values lie above the total (direct) ionization cross-sections $Q(H_2O^+)$ of Srivastava [14], as it should be. The grand-total cross-sections Q_{TOT} are obtained incoherently through (4).

We now discuss the results of the present calculations in terms of the analytical fits given in (5) and (8). Consider figure 1 which shows the graphical representation of the fitting formula of (5) for $e^- - H_2O$ scattering. Both the present Q_{inel} as well as the experimental $Q(H_2O^+)$ plotted here, are found to obey this relation at high energies (above 100 eV) and yield straight lines with an identical slope $M_{tot}^2 = 4\cdot28$. This quantity is related to the optical oscillator strength of the molecule. The present value of M_{tot}^2 differs from that in an earlier calculation [20] wherein the ionization energy is taken in place of Δ_{gap}.

Let us next consider our results on the grand total cross-sections Q_{TOT} calculated for the energy range $E_i = 50$–2000 eV. In figure 2, these cross-sections are plotted as functions of energy, and compared with some of the experimental data. For H_2O, our theoretical results are now in a very good agreement with the measurements of Zecca *et al* [4] throughout the present energy range. The experimental data of Sueoka *et al* [3] available up to 300 eV are on the lower side. Thus the present results are in a good general accord with the relevant experiments, and the modifications done here over paper I are meaningful.
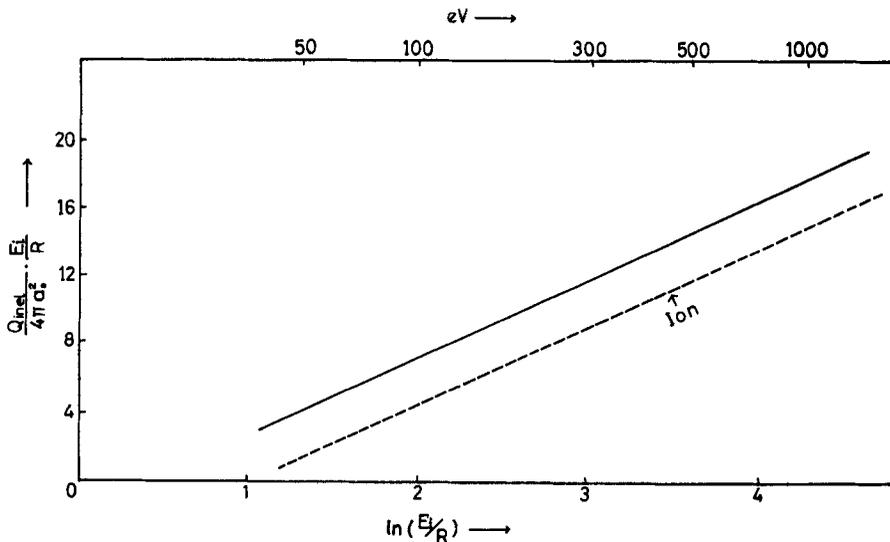
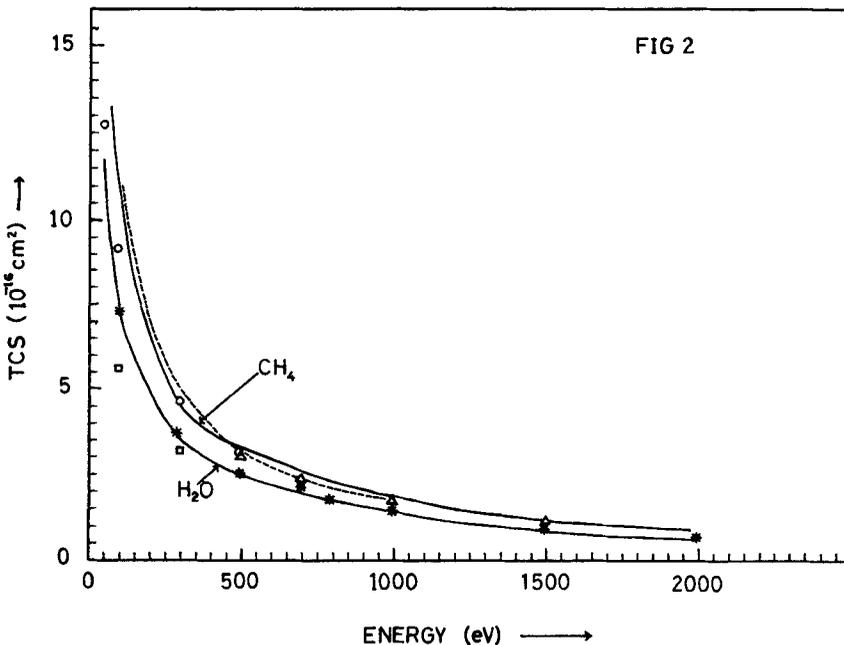**Figure 1.** Bethe plots for H_2O. ———— present Q_{inel}; — — — experimental $Q(H_2O^+)$, vide ref. [14].

Figure 2. Total (elastic + inelastic) cross-sections at various energies. Lower curve———— present H_2O results. (□ Sueoka *et al* [3], ∗ Zecca *et al* [4]). Upper curve——— represents our results for CH_4 (eq. 9), — — — Jiang *et al* [19]. Experimental data for CH_4: ○ Dababneh *et al* [21], △ Zecca *et al* [16].

Table 1. The fitting parameters of eq. (8).

System	a	b	Polarizability Å³
H_2O	239·94	0·742	1·45
NH_3	307·25	0·753	2·26
CH_4	352·24	0·757	2·59

We next examine the energy dependence of the total cross-sections of iso-electronic systems H_2O, NH_3 and CH_4, in the energy range 100–1000 eV. For this purpose we calculated the Q_{TOT} for NH_3 and CH_4 by employing (9). In figure 2 the cross-sections of only H_2O and CH_4 are shown, for simplicity. For CH_4 our results compare favourably with other theoretical [19] as well as experimental [16, 21] results. Now the present results are fitted to the analytical formula of (8). The constants 'a' and 'b' for the present targets are given in table 1. Here Q_{TOT} is in 10^{-16} cm² and E_i is in eV.

We observe from table 1 that all the three 10-electron systems exhibit a similar dependence of Q_{TOT} viz., $(E_i)^{-0.75}$, since 'b' is practically the same for all of them. The other parameter, 'a' is different for each of these molecules and appears to depend on their polarizability α_0. This is clear from the polarizabilities given in table 1. With the parameters given here, eq. (8) very accurately reproduces our theoretical results for all the three molecules in the energy range 100–1000 eV. A similar analysis should be extended to HF molecule, which also has 10 electrons.

Thus in this paper we have considered some more aspects of total electron scattering cross-sections of H_2O at intermediate and high impact energies. Our previous results are now improved and extended to facilitate further studies. Our total inelastic cross-sections are consistent with the measured ionization cross-sections, barring dissociative ionization. Our Q_{inel} values obey the well-known Bethe formula, (5). As regards the total cross-sections Q_{TOT}, systematic relations are confirmed here for the target sequence H_2O–NH_3–CH_4. At a fixed E_i the cross-sections increase along this sequence, but tend to merge at high enough energies. The present results follow the energy dependence given through (8) and table 1.

It would be desirable to consider accurate *ab initio* charge-densities and corresponding static-exchange potentials in *e*-molecule scattering.

Acknowledgement

References

[1] K N Joshipura, Minaxi Vinodkumar and P M Patel, *Pramana – J. Phys.* **43**, 495 (1994)
[2] G Staszewska, D Schwenke, D Thirumalai and D G Truhlar, *Phys. Rev.* **A28**, 2740 (1983)
[3] O Sueoka, S Mori and Y Katayama, *J. Phys.* **B19**, L373 (1986); *J. Phys.* **B20**, 3237 (1987)
[4] A Zecca, G P Karwasz, S Oss, R Grisenti and R S Brusa, *J. Phys.* **B20**, L133 (1987)

[5] M T Lee, S E Michelin, T Kroin, L E Machado and L M Brescansin, *J. Phys.* **B28**, 1859 (1995)
[6] T Nishimura and Y Itikawa, *J. Phys.* **B28**, 1995 (1995)
[7] A Katase, K Ishibashi, Y Matsuomoto, T Sakae, S Maezono, E Murakami, K Watanabe and H Maki, *J. Phys.* **B19**, 2715 (1986)
[8] K B Ghose and S Pal, *J. Chem. Phys.* **99**, 945 (1993)
[9] S Pal, K B Ghose and H Meyer, *Int. J. Quant. Chem.* **55**, 291 (1995)
[10] K E Banyard and N H March, *J. Chem. Phys.* **26**, 1416 (1957)
[11] D G Thompson and F A Gianturco, *Chem. Phys. Lett.* **14**, 110 (1976)
[12] Arvind Jain, A N Tripathi and Ashok Jain, *Phys. Rev.* **A37**, 2893 (1988)
[13] M Inokuti, *Rev. Mod. Phys.* **43**, 297 (1971)
[14] S K Srivastava, private communication (1995)
[15] H Nishimura and H Tawara, *J. Phys.* **B24**, L363 (1991)
[16] A Zecca, G P Karwasz and R S Brusa, *Phys. Rev.* **A45**, 2777 (1992)
[17] Minaxi Vinodkumar, P M Patel and K N Joshipura, *Prajna – J. Sardar Patel University*, **5**, 79 (1995)
[18] K N Joshipura and P M Patel, *Z. Phys.* **D29**, 269 (1994)
[19] Y Jiang, J Sun and L Wan, *Phys. Rev.* **A52**, 398 (1995)
[20] A Jain and K L Baluja, *Phys. Rev.* **A45**, 202 (1992)
[21] M S Dababneh, Y F Hsieh, W E Kauppila, C K Kwan, S J Smith, T S Stein and M N Uddin, *Phys. Rev.* **A38**, 1207 (1988)